Construction and Building Materials 108 (2016) 56–66

Contents lists available at ScienceDirect

Construction and Building Materials

journal homepage: www.elsevier.com/locate/conbuildmat

Influence of service loading and the resulting micro-cracks on chloride resistance of concrete

Junjie Wang [a], P.A. Muhammed Basheer [b,*], Sreejith V. Nanukuttan [a], Adrian E. Long [a], Yun Bai [c]

[a] School of Planning, Architecture and Civil Engineering, Queens University of Belfast, Northern Ireland, UK
[b] School of Civil Engineering, University of Leeds, England, UK
[c] Department of Civil, Environmental & Geomatic Engineering, University College London, England, UK

HIGHLIGHTS

- Effect of microcracks due to sustained loading on chloride transport into concrete was obtained.
- Stress levels above 50% of the ultimate can cause a great increase in chloride ingress.
- Mineral additives perform well against chloride ingress in concrete subjected to sustained loading.
- At high stress levels, removal of the load results in a recovery of the chloride resistance.

ARTICLE INFO

Article history:
Received 30 July 2015
Received in revised form 25 December 2015
Accepted 5 January 2016
Available online 28 January 2016

Keywords:
Chloride transport
Service life
Micro-cracks
Load effect
Stress level

ABSTRACT

Chloride-induced corrosion of steel in reinforced concrete structures is one of the main problems affecting their durability, but most previous research projects and case studies have focused on concretes without cracks or not subjected to any structural load. Although it has been recognised that structural cracks do influence the chloride transport and chloride induced corrosion in reinforced concrete structures, there is little published work on the influence of micro-cracks due to service loads on these properties. Therefore the effect of micro-cracks caused by loading on chloride transport into concrete was studied. Four different stress levels (0%, 25%, 50% and 75% of the stress at ultimate load – f_u) were applied to 100 mm diameter concrete discs and chloride migration was measured using a bespoke test setup based on the NT BUILD 492 test. The effects of replacing Portland cement CEMI by ground granulated blast-furnace slag (GGBS), pulverised fuel ash (PFA) and silica fume (SF) on chloride transport in concrete under sustained loading were studied. The results have indicated that chloride migration coefficients changed little when the stress level was below 50% of the f_u; however, it is desirable to keep concrete stress less than 25% f_u if this is practical. The effect of removing the load on the change of chloride migration coefficient was also studied. A recovery of around 50% of the increased chloride migration coefficient was found in the case of concretes subjected to 75% of the f_u when the load was removed.

1. Introduction

Chloride-induced corrosion of steel in reinforced concrete structures is one of the most serious problems affecting their service life and if unattended it can put the infrastructure at risk and endanger people's lives. An understanding of the processes of chloride transport in concrete is very important for engineers attempting to predict the service life of reinforced concrete structures and numerous studies dealing with this topic can be found in the literature [1–9]. However, most of them have focused on concretes which are neither cracked nor subjected to any structural loading. The work by Gowripalan et al. [10] showed that chloride diffusivity of concrete in the compression zone was much smaller than that in the tension zone when concrete beams were subjected to flexure. Win et al. [11] suggested that chloride can readily penetrate into the concrete through an open crack. Other studies on the influence of crack width on chloride transport [12–15] showed that the influence of micro-cracks on chloride ingress can be significant.

Although it has been recognised that structural cracks do influence the chloride transport and chloride induced corrosion of steel in reinforced concrete structures, there is little published work on the influence of micro-cracks due to service loads on these properties. In some studies [12,16–21] chloride transport

* Corresponding author.
E-mail address: p.a.m.basheer@leeds.ac.uk (P.A.M. Basheer).

http://dx.doi.org/10.1016/j.conbuildmat.2016.01.005
0950-0618/

tests on concrete have been conducted after the load was removed, but the results of concrete under loading and after the load is removed can be different. Based on tests conducted under sustained compressive loading, Antoni et al. [22,23] reported a significant increase of chloride transport into plain concrete when the compressive stress level was above 50% of the ultimate stress – f_u. In contrast, based on a numerical simulation a linear decrease of chloride diffusion in concrete under sustained compressive stress from an unloaded state up to 50% f_u was reported by Wang et al. [24]. It was found that some conflicting views exist in the literature on critical stress level and chloride transport properties of concretes under different loading conditions. Further, most of the work focused on concrete containing only Portland cement CEMI [24,25], and data on concrete with mineral additives are still limited.

The existing service life prediction models, such as Life-365 [26,27], AGEDDCA model [28] and DuraCrete [29], do not consider any effect of loading or consequential cracking (macro-cracking or micro-cracking; micro-cracks are defined below as cracks <0.1 mm wide), hence the predicted service life may not be reliable for most structures in service. The effect of stresses and micro-cracks on chloride transport is not considered in the current Standards. The Eurocode 2 [30] restricts the crack width to 0.3 mm for reinforced concrete in chloride-laden environments but has no restrictions on concretes with small cracks (<0.3 mm) or micro-cracks (<0.1 mm). As a consequence, premature deterioration of structures in service is common. For example, on the basis of a field survey of 57 bridges in Kansas, USA, Lindquist et al. [31] have indicated that the chloride concentration at a depth of 76 mm from the location of a surface crack can exceed the corrosion threshold amount within the first year. Another survey of 219 marine structures along the Norwegian coastline has shown that the signs of corrosion could be seen as early as 5–10 years, which means that the time for corrosion initiation was even earlier [32]. Almost all of these structures required major repair at the age of 20 years, which is significantly earlier than their design life of 100 years.

Therefore, the influence of micro-cracks due to structural loads on the chloride transport in concrete was investigated and thereby recommendations for any change of service life designs of such structures are made. As concrete structures exposed to chloride environments are manufactured with cementitious materials containing mineral additives, the effect of such cementitious materials on micro-cracking under sustained loading and its consequential influence on chloride transport were part of the research reported in this paper.

2. Materials and test methods

2.1. Materials

The coarse aggregate used was crushed 5–20 mm well graded basalt (size 5–10 mm 33% and size 10–20 mm 67%) and the fine aggregate was natural medium graded sand conforming to BS EN 12620:2002 [33]. Both types of aggregates were oven-dried at 100 ± 5 °C for 24 h to remove the initial moisture content and then allowed to cool down to room temperature (~18 °C) in air-tight containers before being used. Class 42.5 N Portland cement CEMI conforming to BS EN 197-1:2011 [34] was used. Ground granulated blast-furnace slag (GGBS) complying with BS EN 6699: 1992 [35], pulverised fuel ash (PFA) complying with BS EN 450 [36] and silica fume (SF) conforming to BS EN 13263 [37] were used to replace part of CEMI in the mixes studied.

The proportions for each mix, along with their physical properties, are reported in Table 1. As can be seen from Table 1, some of the mixes were added with a polycarboxylate polymer-based superplasticiser conforming to BS EN 934-2 [38]. The solid content of the superplasticiser was 29%. The water content of superplasticiser was considered to be part of the mixing water and hence this quantity was deducted from the water content reported in Table 1. Water from the mains at a temperature of 20 (±1) °C was used to manufacture all mixes.

2.2. Manufacture of test specimens

Four blocks (250 × 250 × 80 mm) and six 100 mm cubes were cast for each mix. The required quantities of the mix constituents were batched by mass and then mixed using a pan mixer in accordance with BS 1881-125: 1986 [39]. The slump was measured immediately after batching the concrete. The concrete was placed in the moulds in three layers and each layer was compacted using a vibrating table until air bubbles appearing on the surface stopped. The cast surface of each concrete specimen was then finished with a trowel and covered by a thick black polythene sheet to prevent any loss of water. The samples were demoulded after 24 h, they were then placed in a water bath at 20 (±1) °C for 3 days, after which they were wrapped in wet hessian and thick black polythene sheet. The specimens were then placed in a constant temperature room at 20 (±1) °C.

2.3. Test methods

2.3.1. Compressive strength test

The cubes were used to carry out the compressive strength test at an age of 28 and 56 days for each mix, the results of which have already been reported in Table 1.

2.3.2. Chloride migration test

Cores of size 100 mm diameter and 80 mm thickness were cut from the blocks at an age of 56 days and the outermost, approximately 15 mm thick layer, was cut off from the two end surfaces using a water-cooled diamond saw. This was done to eliminate the effects of the boundary layer on chloride transport and ensure a smooth test surface of the samples. The middle part of 50 (±1) mm was thus used as the test specimen. The thickness of each specimen was measured with a digital calliper to an accuracy of 0.1 mm. The chloride migration test was carried out using these disks. In order to test them under sustained loading, they were compressed by two diametrically opposite loads by using a special setup that was designed and manufactured, as shown in Figs. 1 and 2. This test setup is novel in the sense that it was not used before and was designed to stimulate micro-cracking of reinforced concrete under the sustained loading condition.

Samples were saturated as per the preconditioning procedure outlined in NT BUILD 492 [40]. The cores were placed in a vacuum container after they were surface-dried, by making sure both end surfaces were exposed. The pressure inside was reduced to 30 (±5) mbar and the vacuum was maintained for three hours. Then the container was filled with $Ca(OH)_2$ solution to immerse all specimens, with the pump still running. The vacuum was maintained for a further hour before allowing air to enter. The cores were kept in the solution for another 18 h, after which they were taken out for placing in the test setup. The cores were then coated on the curved surface with a silicon coating material and clamped in position (Fig. 2). After the silicon had hardened, the specimens were loaded at a constant rate of 1.23 (±0.1) kN/s until failure. The average load of the three failure loads in each mix was taken as the maximum load and the related stress was taken as the ultimate stress – f_u for each mix. The typical crack pattern at the failure of the core specimen is shown in Fig. 3.

Three loading conditions (Control – no loading, under loading and after unloading) were utilised. Fig. 4 shows that cores under different loading conditions were treated separately before testing. The load was removed after 1 min of loading for the After Unloading condition and UPV tests were conducted before the load was applied and after the load was removed. The load was kept constant throughout the test period for the under loading condition, UPV tests were conducted before and after the load was applied. No load applying and UPV tests for the Control condition. Different stress levels (equivalent to 25%, 50%, and 75% of f_u) were applied to the cores by fastening the nuts at the top of the brackets using a torque wrench. Strain gauges placed on bolts were used to determine the forces in the bolts, indicated in Fig. 2. An ultrasonic pulse velocity (UPV) test was conducted before and after the load was applied.

- Control: Specimens were ready for testing and no UPV test was conducted.
- Under loading: Different levels of load were applied and maintained for the tests conducted. An UPV test was conducted before and after the load was applied.
- After unloading: Different levels of load were applied and kept constant for 1 min, and then the load was released. UPV tests were conducted before applying and after releasing the load.

As shown in Fig. 3, cracks along the direction of loading were formed when the cores were under a certain load. The ultrasonic pulse velocity (UPV) in 3 different directions (Fig. 5) was used to determine the damage degree θ, which is the change in UPV [41] as per Eq. (1) caused by the loading. As illustrated in Fig. 5, a direct method and two indirect methods were used to measure the UPV for all mixes. Exactly the same locations were utilised before and after each load was applied and vaseline petroleum jelly was used as a couplant between the transducer and the concrete surface. The transducers with a frequency of 54 kHz were pressed by

Table 1
Concrete mix proportions and physical properties.

Mix	Portland cement	GGBS	PFA	SF	Water	Super-plasticiser	Coarse aggregate	Sand	Slump	Compressive strength	
										28 d	56 d
	kg/m^3								mm	MPa	
0.45-CEMI	300	–	–	–	135	0.39	1238	825	100	58.7	60.2
0.45–10%SF	270	–	–	30	135	0.52	1230	820	106	59.6	67.5
0.45–35%GGBS	195	105	–	–	135	0.44	1233	826	105	49.8	62.3
0.65-CEMI	300	–	–	–	195	–	1142	761	95	37.8	38.7
0.65–10%SF	270	–	–	30	195	0.22	1134	756	125	39.2	49.8
0.65–35%PFA	195	–	105	–	195	–	1117	744	120	29.2	38.3
0.65–35%GGBS	195	105	–	–	195	–	1137	758	100	35.1	48.9
0.65–65%GGBS	105	195	–	–	195	–	1133	755	115	33.5	40.6

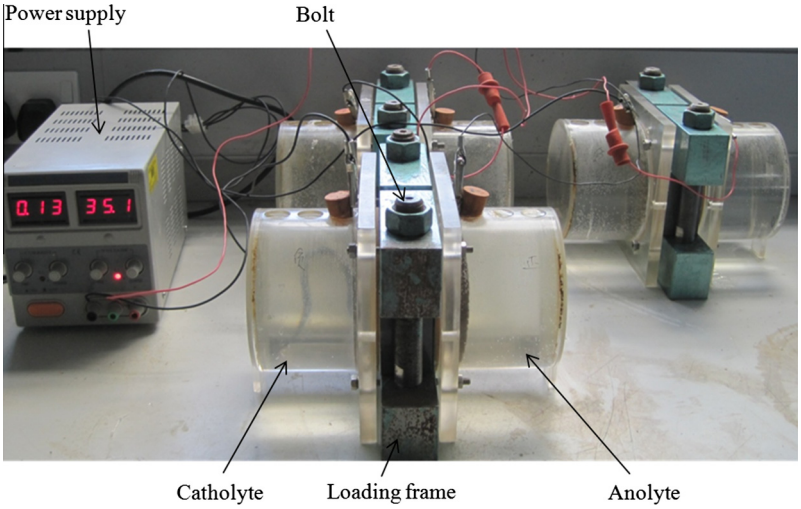

Fig. 1. Setup for carrying out migration test under sustained loading.

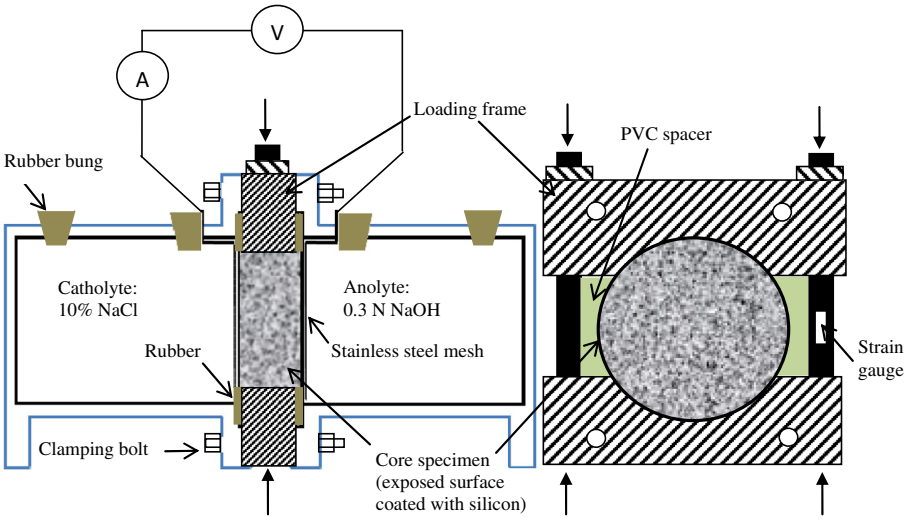

Fig. 2. Schematic setup of the chloride migration test of concrete under loading.

hand at a constant force against the concrete surface to ensure good acoustical contact. Repeated readings at each location were taken and the minimum transit time was reported. After each test, the concrete surface was polished by means of a sand paper so as to avoid any jelly being left on the surface.

$$\theta = \frac{V_0 - V}{V_0} \quad (1)$$

where θ is the damage degree calculated from the change in UPV before and after loading; V_0 and V are UPV measured at the same location in the concrete specimen before and after loading was applied; L is the measured distance between the two transducers.

All cores were tested for chloride transport in accordance with the NT BUILD 492 test procedure [40]. In the condition of 'under loading', rubber rings and spacers were fitted on the cores to prevent any leakage. The rubber ring also served to

Fig. 3. Typical cracks formed when a core specimen was compressed to failure on its curved surface.

prevent any direct contact between the solution in each cell and the metal frame in order to avoid the passage of direct current through the metal frames. The end surface nearer to the as-cast surface was the one exposed to the chloride solution (catholyte). The catholyte reservoir was filled with 10% (by mass) NaCl solution and the anolyte reservoir with 0.3 M NaOH solution (in de-ionised water). The electrodes were connected to the power supply and the test voltage was selected according to NT BUILD 492 [40]. At the end of the test the cores were taken out of the frame and split into two halves along the cracks in the same direction of loading in order to make use of the worst case of chloride penetration for calculating the chloride migration coefficient (highest chloride penetration was expected to be along the crack, but splitting perpendicular to the cracks would have produced different chloride migration coefficients). The chloride migration coefficient was determined according to Eq. (2) [40]. For each test 3 replicates were tested and the average value was determined.

$$D_{nssm} = \frac{0.0239(273+T)L}{(U-2)t}\left(x_d - 0.0238 * \sqrt{\frac{(273+T)Lx_d}{U-2}}\right) \quad (2)$$

where D_{nssm} ($\times 10^{-12}$ m^2/s) is a non-steady state chloride migration coefficient obtained from a non-steady state migration test, U (V) is the absolute value of the applied voltage, T (°C) is the average value of the initial and final temperatures in the anolyte solution, L (mm) is the thickness of the specimen, x_d (mm) is the average value of the penetration depth and t (hour) is the test duration.

3. Results and discussion

3.1. Influence of service loading on D_{nssm}

Fig. 6 shows a case of typical changes in D_{nssm} due to the applied load. There is almost no change of D_{nssm} when the stress level increased to 25% f_u; above this level and up to 50% f_u, D_{nssm} increases a little; with the stress level increasing up to 75% f_u, a significant increase of D_{nssm} is obtained. No visible cracks were observed in any of the specimens after testing.

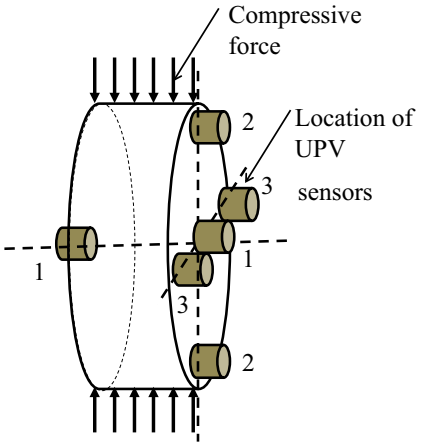

Fig. 5. Different directions of measuring ultrasonic pulse velocity through concrete. *Note:* 1–1 along crack inside concrete, 2–2 parallel with crack direction on surface of concrete, 3–3 perpendicular to crack direction on surface.

Mehta and Monteiro [42] have suggested that there is no change in behaviour of concrete up to 30% of the ultimate stress, slight damage to the structure between 30% and 50% of the ultimate stress, significantly increased damage between 50% and 75% of the ultimate stress, and the system becomes unstable beyond 75% of the ultimate stress. The changing behaviour of D_{nssm} of 0.65-CEMI concrete presented in Fig. 6 agrees well with the crack developing stages of CEMI concrete under compressive loading suggested by Mehta and Monteiro [42]. Below 25% f_u is within the elastic range of concrete, and there is no development of microcracks. Around 50% f_u, there is a stable development of microcracks in the interfacial transition zone. Up to 75% f_u, cracks begin to form and increase in the matrix and the crack system in the interfacial transition zone becomes unstable. Sustained loading above 75% f_u should be avoided because the crack systems of concrete become extremely unstable and can easily fail [42].

As shown in Fig. 6, a significant difference can be found between the values of D_{nssm} in concretes before and under loading. Concrete structures have to sustain service loading, such as live and dead loads; therefore, the stress level is an important factor to consider in the context of chloride ingress. The effect of loading on chloride ingress into concrete can be considered in the design stage of reinforced concrete structures if the range of the actual stresses on the structure is known.

Typical relationships between characteristic values and design values of the concrete strength and the stress are shown in Fig. 7. The maximum stress level of concrete according to the design standard Eurocode 2 can be estimated as f_d/f_{ck}.

BS EN 1992-1-1:2004 [30] defines the value of design compressive strength (f_{cd}) as Eq. (3).

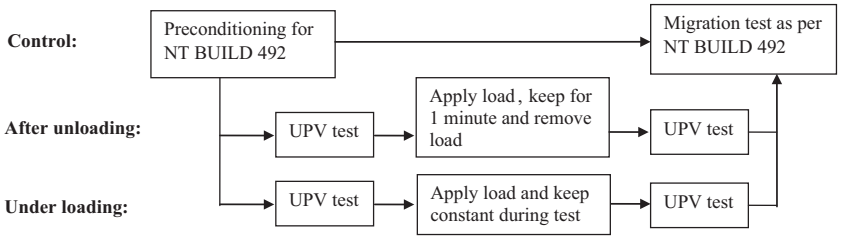

Fig. 4. Flow chart for tests conducted on three loading conditions.

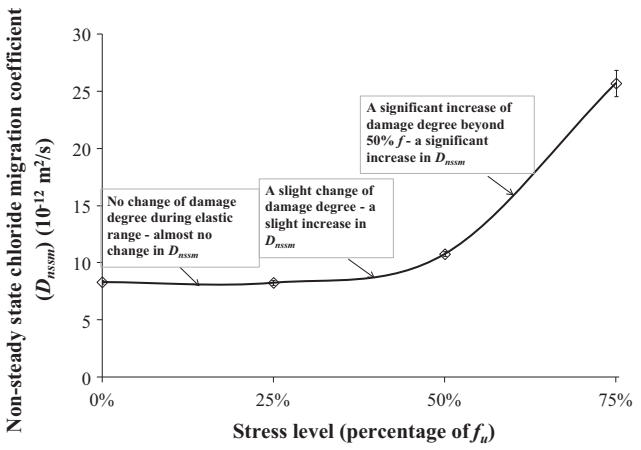

Fig. 6. Relationship between stress level applied and non-steady state chloride migration coefficient for 0.65-CEMI concrete.

$$f_{cd} = \alpha_{cc} f_{ck} / \gamma_C \quad (3)$$

where f_{ck} is the characteristic compressive strength of concrete; α_{cc} (=0.85) is the coefficient taking account of long term effects on the compressive strength and of unfavourable effects resulting from the way the load is applied; γ_C is the partial safety factor for concrete, $\gamma_C = 1.5$ for persistent and transient design situation which is 1.2 for accidental situation [43].

Then the maximum design stress level of in-service concrete can be calculated as in Eqs. (4) and (5).

Persistent and transient (normal loading condition):

$$\frac{f_{cd}}{f_{ck}} = \frac{\alpha_{cc}}{\gamma_c} = \frac{0.85}{1.5} = 57\% \quad (4)$$

Accidental (unusual loading condition):

$$\frac{f_{cd}}{f_{ck}} = \frac{\alpha_{cc}}{\gamma_c} = \frac{0.85}{1.2} = 71\% \quad (5)$$

From the above calculation, the normal stress level is around 57% f_u and the accidental stress level is around 71% f_u, as shown in Fig. 8. Stress levels discussed here are related to design loads; in service, real loads are lower due to the use of partial safety factors in design. Further, real loads and stresses also depend on live to dead load ratios.

It can be seen from Fig. 6 that D_{nssm} of concrete, within the range of stress levels 57% and 71% f_u could increase by 100–200% of that without loading. Thus the service life predicted, based on concrete in unloaded state, might be too optimistic, which suggests that the actual service loading should be considered for the durability design stage.

3.2. Influence of mix variables on D_{nssm}

3.2.1. Influence of w/b on D_{nssm}

Fig. 9 shows the relationship between D_{nssm} and the stress level for each concrete mix. The D_{nssm} values might be lower than some of the published data, but the overall quality of the data is good and the difference between mixes is clear. As one would expect, the w/b has a significant influence on D_{nssm} for each type of concrete (i.e. binder type). The value of D_{nssm} of 0.45-CEMI and 0.45–10%SF is much lower than that of 0.65-CEMI and 0.65–10%SF respectively. This is because concrete with a higher w/b has a higher porosity as well as higher percolation.

Fig. 10 shows the relationship between D_{nssm} and the actual value of the load applied for each concrete mix. The change in chloride migration coefficient for each mix due to the application of 43 kN (highest load that was resisted by the 0.65-CEMI concrete) is reported in Table 2. The load 43 kN was selected because D_{nssm} for all mixes are available under this load. Also reported are the changes in chloride migration coefficient due to approximately half of 43 kN (≅20 kN) applied to the samples. The highest increase of 208% is for the 0.65-CEMI concrete subjected to 43 kN. In comparison, the increase for the 0.45-CEMI concrete at 43 kN load was only 22%. This is because concrete with a lower w/b has a higher strength (and hence higher tensile resistance) and can withstand higher load before D_{nssm} begins to increase.

3.2.2. Influence of types of binder on D_{nssm}

As shown in Fig. 9, the curves of D_{nssm} under different stress levels for both PFA and GGBS concretes are quite similar, but they are different from that of the CEMI concretes. The addition of PFA and GGBS resulted in an almost no change in D_{nssm}. The SF concretes on the other hand show a trend similar to that of CEMI concretes, but the overall values of D_{nssm} are greatly decreased. These results suggest that the addition of PFA, GGBS and SF is beneficial to control the chloride ingress for concrete structures under sustained loading.

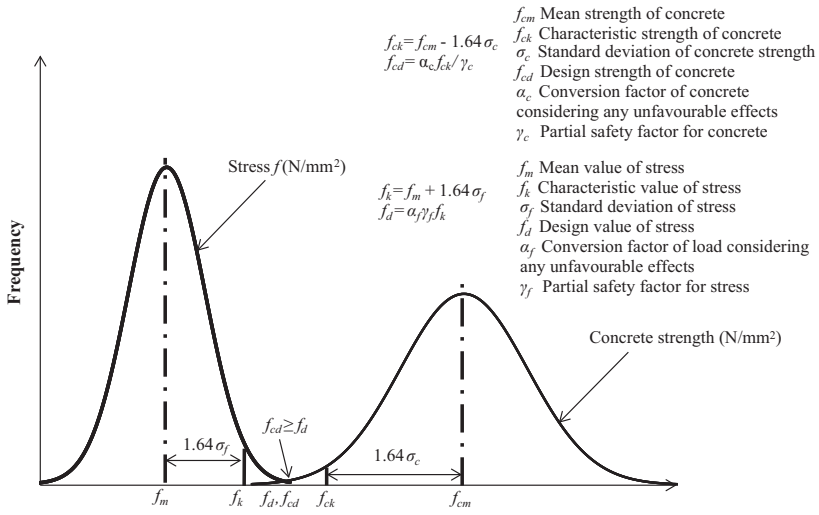

Fig. 7. Relationship between characteristic values and design values for both the concrete strength and the stress in concrete.

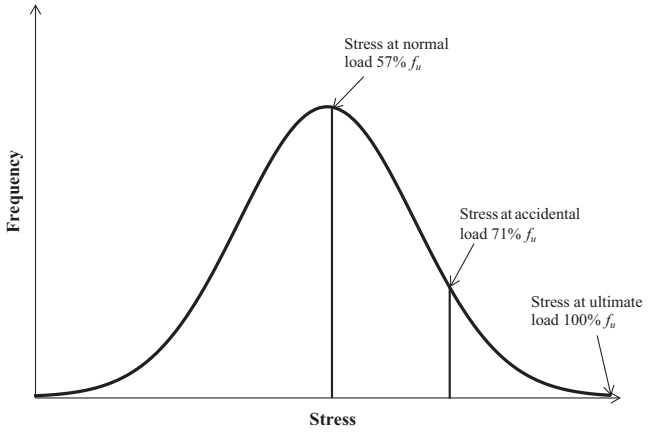

Fig. 8. Stress levels under normal load and accidental load.

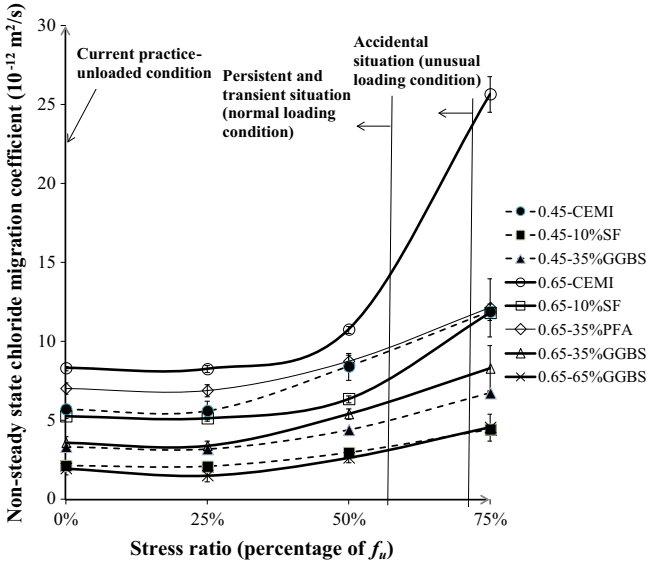

Fig. 9. Relationship between stress level applied and chloride migration coefficient for different concrete mixes.

From Table 2, it can be seen that at 43 kN sustained load, 0.65-CEMI concrete has a very high increase in D_{nssm} and both 0.65–35% PFA and 0.65–10%SF concretes have lower increases. However, under the same load, 0.65–35%GGBS and 0.65–65%GGBS concretes had a very low increase and even a decrease in D_{nssm}. The data in Table 2 were calculated based on curve fitting done to the measured data because actual data points were not available for both 43 kN and 20 kN for all mixes except 0.65-CEMI. As a result, no attempt is made to test for statistical significance of the effects reported in Table 2. D_{nssm} of 0.65-CEMI increased rapidly with increasing force applied due to relatively lower strength of this concrete. However, there was little change for 0.65–35%GGBS and 0.65–65%GGBS concretes with the same range of load applied. Thus, the binder type is an important factor to consider for the durability of concrete under service loads.

3.3. Model of D_{nssm}

In structural design, the effect of uncertainties of loads is taken into account by using a partial safety factor. A similar approach can be used in the case of chloride transport as well. From the above analysis, the D_{nssm} of concrete under loading can be described as

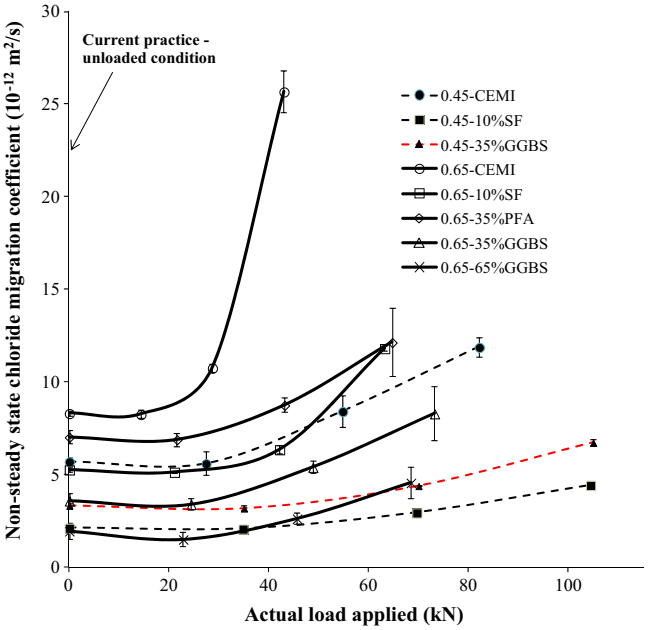

Fig. 10. Relationship between the applied load and chloride migration coefficient for different concrete mixes.

Table 2
Percentage increases in chloride migration coefficient for each mix due to sustained application of 20 kN and 43 kN loads.

Mix	0 kN	20 kN		43 kN	
	D_{nssm}	D_{nssm}	Percentage (%)	D_{nssm}	Percentage (%)
0.45-CEMI	5.72	5.5	−4	7	22
0.45–35%GGBS	3.53	3.4	−4	3.5	−1
0.45–10%SF	2.14	2.0	−7	2.3	+7
0.65-CEMI	8.33	9.2	+10	25.68	+208
0.65–35%GGBS	3.61	3.3	−9	3.9	+8
0.65–65%GGBS	1.97	1.5	−24	1.7	−14
0.65–35%PFA	7.04	6.9	−2	8.7	+24
0.65–10%SF	5.28	5.4	2	6.4	+21

D_{nssm0} (without loading) multiplied by a factor of λ_L, as shown in Eq. (6). λ_L is related to w/b, stress level (f/f_u) and mineral additives (ma). The work of Buenfeld and Okundi [44] suggests that the effect of binder content (cc) should be included in such modelling. Thus λ_L can be described by a function given in Eq. (7).

$$D_{nssm} = D_{nssm0} \cdot \lambda_L \tag{6}$$

$$\lambda_L = f(w/b, f/f_u, ma, cc) \tag{7}$$

Note that λ_L will always be $\geqslant 1$. $\lambda_L < 1$ should be taken as 1 for safety reasons. The data reported in this paper is not sufficient to establish the function λ_L in terms of the parameters in Eq. (7).

3.4. Effect of unloading on D_{nssm} of concretes

Fig. 11 shows the effect of unloading from different stress levels on the change of D_{nssm} of each mix. The effects of loading and unloading on changes in chloride migration coefficient of each mix are reported in Table 3. Changes below 20% are not considered to be statistically significant and this suggests the load levels below 50% f_u do not have a significant effect on chloride penetration resistance of concrete. It can be seen clearly from Fig. 11 that there is a significant recovery after the load was removed. The change of D_{nssm} at 25% f_u (elastic range of concrete) was fully recovered when the load was released, but only a part of the increase in D_{nssm} due to

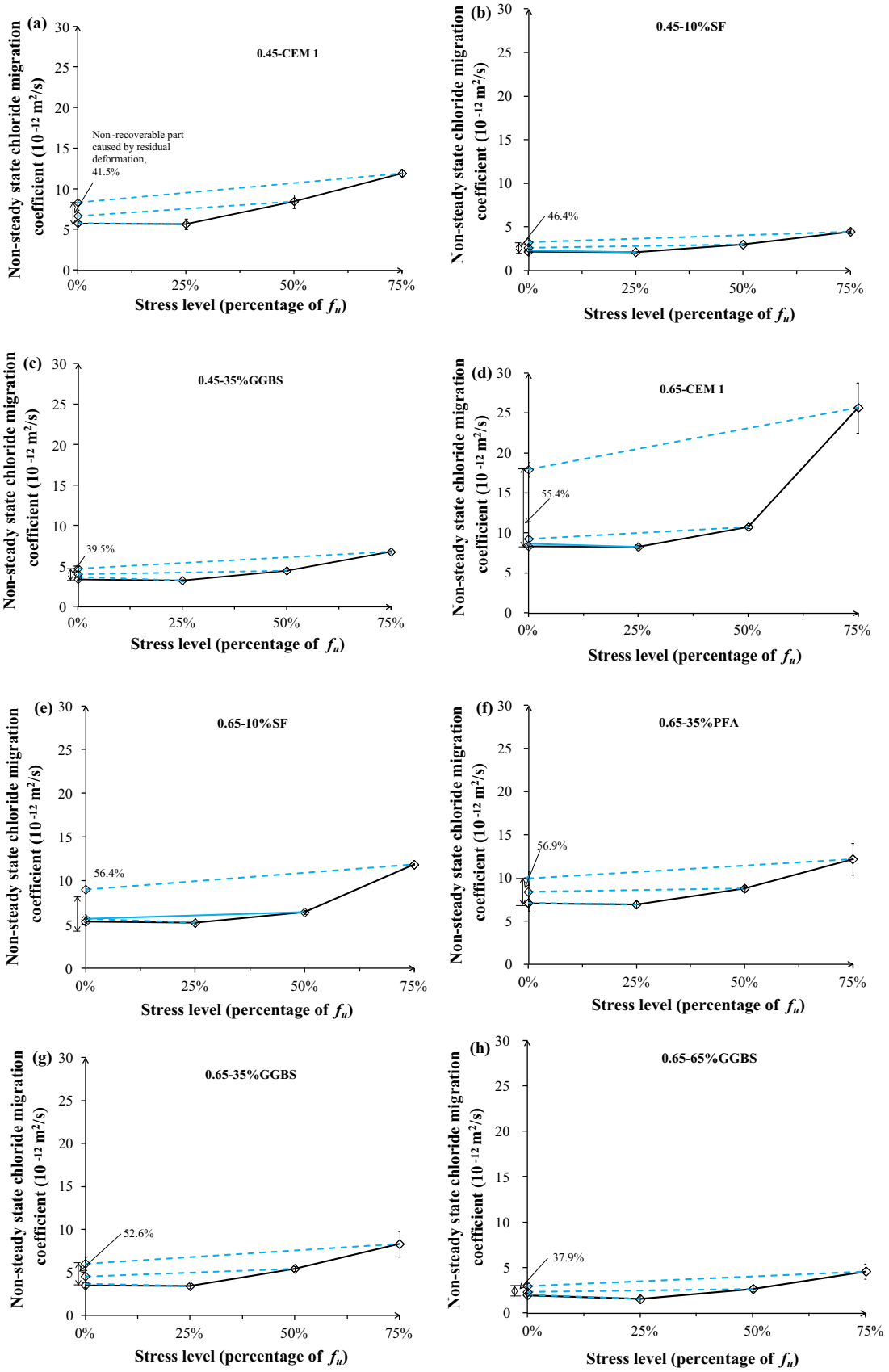

Fig. 11. (a–h) Non-steady chloride migration coefficients of concretes under sustained loading and after unloading from different stress levels (the additional data points at 0% load are the results of testing after first loading to each load level and then unloading).

Table 3
Percentage change in chloride migration coefficient for each mix due to sustained loading and unloading (compared with no load condition).

Mix	Under loading			After unloading		
	25% f_u	50% f_u	75% f_u	25% f_u	50% f_u	75% f_u
0.45-CEMI	−2%	+47%	+108%	+1%	+16%	+45%
0.45–35%GGBS	−4%	+32%	+101%	+10%	+19%	+40%
0.45–10%SF	−2%	+39%	+108%	+7%	+21%	+50%
0.65-CEMI	−1%	+29%	+208%	+4%	+11%	+115%
0.65–35%GGBS	−5%	+50%	+130%	+1%	+26%	+67%
0.65–65%GGBS	−22%	+34%	+132%	+2%	+17%	+50%
0.65–35%PFA	−2%	+24%	+73%	+1%	+19%	+41%
0.65–10%SF	−2%	+21%	+124%	+7%	+7%	+70%

Table 4
The increase in D_{nssm} due to short-term loading and its recovery after unloading for 50% f_u and 75% f_u.

Mix group	50% f_u		75% f_u	
	Increase* (%)	Recovery* (%)	Increase* (%)	Recovery* (%)
0.45-CEMI	16	66	45	58
0.45–35% GGBS	19	41	40	60
0.45–10%SF	21	45	50	54
0.65-CEMI	11	61	115	45
0.65–35% GGBS	26	49	67	49
0.65–65% GGBS	17	50	50	62
0.65–35%PFA	19	22	41	43
0.65–10%SF	7	66	70	44

* Note: Increase = $(D_{nssm\text{-}after\ unloading} - D_{nssm0})/D_{nssm0}$. Recovery = $(D_{nssm\text{-}under\ loading} - D_{nssm\text{-}after\ unloading})/(D_{nssm\text{-}under\ loading} - D_{nssm0})$. D_{nssm0} is chloride migration coefficient of concrete with no loading; $D_{nssm\text{-}under\ loading}$ and $D_{nssm\text{-}after\ unloading}$ are chloride migration coefficients of concretes under loading and after unloading respectively.

sustained load was recovered when the load was $\geqslant$50% f_u, which might have been caused by the presence of residual cracks [42].

The increase and recovery of D_{nssm} for each mix after unloading from 50% f_u and 75% f_u are compared and summarised in Table 4.

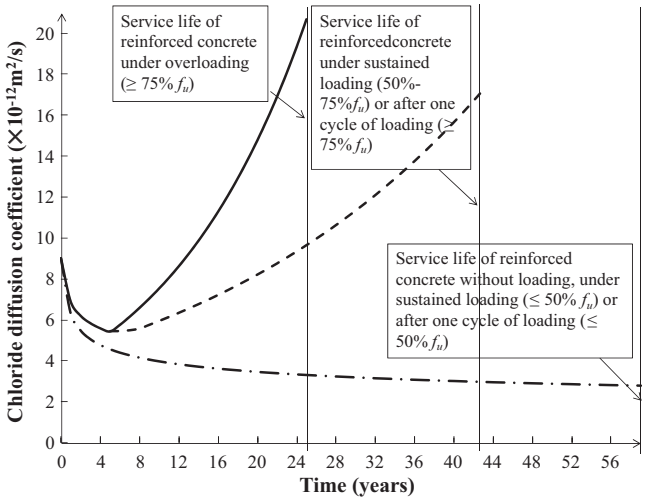

Fig. 13. Change of chloride diffusion coefficient of concrete with time under service loading and corresponding service life for 0.65-CEMI concrete.

D_{nssm} significantly decreased after the load 75% f_u was removed and the recoverable part is about 50%. This suggests that the short-time loading might not cause a lasting detrimental effect on the chloride penetration resistance of concrete structures. The non-recoverable part might increase with the frequency of loading when concrete suffers cyclic loading [20,45], which is an important topic to consider for structures subjected to traffic, wind and earthquake loads.

3.5. Service life of concretes for different stress levels

Life 365 v2.1 [27] was used to calculate the service life of the reinforced concrete element under assumed different stress levels. A square reinforced concrete column with a cover depth of 60 mm was assumed to be exposed in the tidal zone of the North Sea at Dornach in Scotland, where the data of the temperature and surface chloride content was collected [46]. It was assumed that the

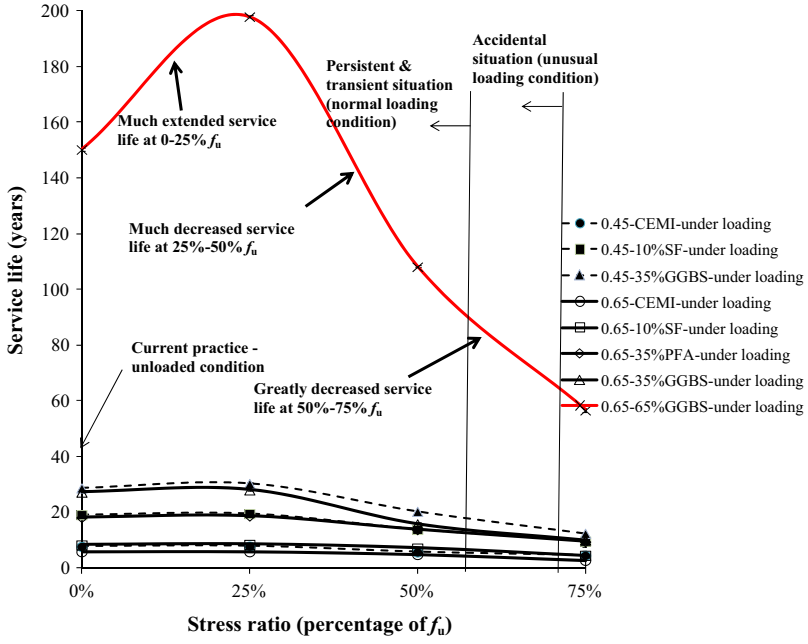

Fig. 12. Service life calculated using Life 365 for concrete under service loading.

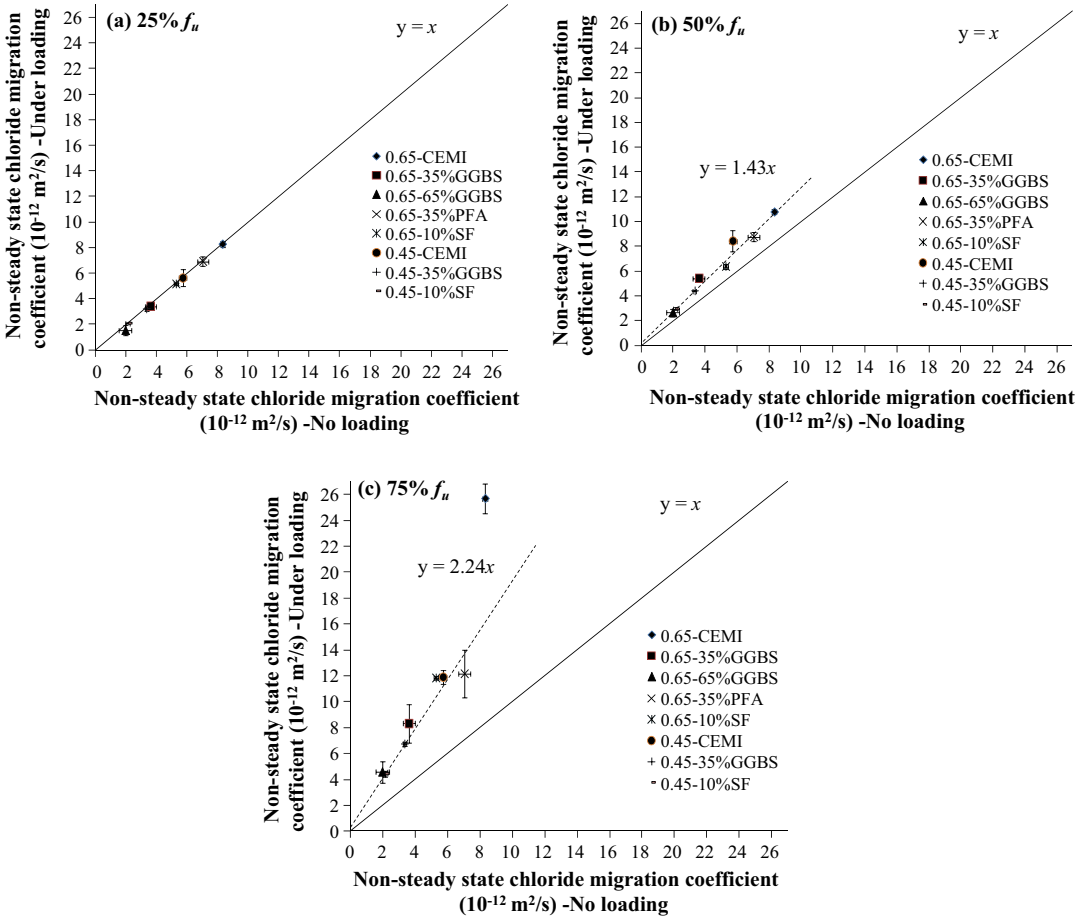

Fig. 14. (a–c) Relationship between D_{nssm} of concrete under different stress levels and no loading.

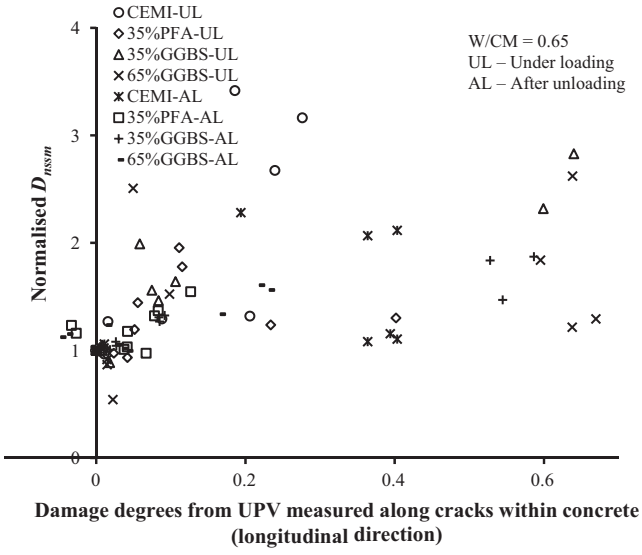

Fig. 15. Relationship between damage degrees based on UPV measured along cracks within concrete (longitudinal direction, i.e. 1–1 in Fig. 5) and normalised D_{nssm}.

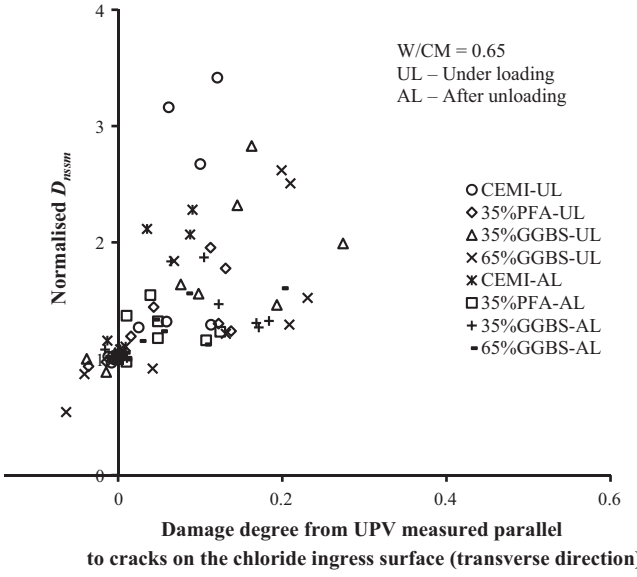

Fig. 16. Relationship between damage degrees based on UPV measured parallel to cracks on the chloride ingress surface (transverse direction, i.e. 2–2 in Fig. 5) and normalised D_{nssm}.

load applied to the column resulted in the same level of stress in the concrete cover as in the interior. Similarly, it was assumed that the effect of a short term load (as studied) is the same as of a sustained load (as in the field). The time needed to build to maximum surface chloride concentration of 0.95% (weight of concrete) was assumed to be 5 years [46]. The reported diffusivity reduction factor (m) in literatures for concrete with 30% PFA was 0.66–0.7 [3,47] and for concrete with 60–70% GGBS was 0.621–1.23 [48]. The max-

imum value of m in Life 365 is 0.6 [27], thus, values of m for different types were assumed as: m = 0.5 for 35% PFA concretes, m = 0.6 for 65% GGBS concretes, m = 0.4 for 35% GGBS concretes and m = 0.2 for CEMI concretes. The default hydration time (25 years) and critical chloride content (0.05% of concrete by weight) were used. Only the corrosion initiation time was considered for the service life calculation. There are limitations on these assumptions. One limitation is to relate the result of discs to the columns on site because of their different stress distributions.

Fig. 12 shows significant differences in service life predicted between concretes without loading and under loading. Service life of concretes under loading at above 75% f_u could be less than half of that without loading. In all the 8 mixes, 0.65–65%GGBS concrete has the best performance with the longest service life at 25% f_u. By adding GGBS, the service life of 0.65–65%GGBS at 75% f_u is still much longer than that of any other mix under loading or without loading, which suggests that adding mineral additives might be a better way to control the detrimental effect caused by loading level in durability design of concrete structures.

A simplified model of the service life of reinforced concrete under different loading conditions based on the data of this research is shown in Fig. 13. The chloride diffusion coefficient changes with time. It may decrease in the first one or two years due to continuous hydration [3,47,49], but then may increase with time because of micro-cracks caused by the service loading. The assumed service lives of reinforced concretes (0.65-CEMI) in different loading conditions are indicated in Fig. 13. As can be seen, it is not appropriate to predict the service life of reinforced concrete without considering the effect of loading, which is not the current practice. High levels of loading (>50% f_u) may significantly reduce the service life of concrete structures.

3.6. Relationships between D_{nssm} of concrete with no loading, under loading and after unloading

Fig. 14 shows the relationship between D_{nssm} of concrete under loading and no loading. All types of concrete show similar behaviour with a higher variation at 75% f_u. D_{nssm} of concrete under 25% f_u is almost the same as D_{nssm} of concrete with no loading, D_{nssm} of concrete under 50% f_u is around 1.43 times of that with no loading and D_{nssm} of concrete under 75% f_u is around 2.24 times of that with no loading. D_{nssm} of concrete under loading can be estimated from these relationships and adjustments to the service life based on no-load condition can be made.

3.7. Relationship between normalised D_{nssm} and damage degree measured by UPV method

Figs. 15–17 show the relationship between damage degrees measured in 3 different directions (Fig. 5) and normalised D_{nssm}. D_{nssm}/D_{nssm0}, where D_{nssm0} is D_{nssm} of concrete without loading, was taken as normalised D_{nssm}. In Fig. 15, the damage degrees obtained from the UPV measurement along the cracks (1–1 in Fig. 5) are plotted against the normalised D_{nssm}. As is evident from this figure, there was no relationship between them for the range of concretes tested for the two loading conditions. A similar finding was obtained in Fig. 16, which shows the damage degrees based on UPV measured parallel to the cracks on the test surface (2–2 in Fig. 5) and the normalised D_{nssm}. However, in Fig. 17, there is an exponential relationship between the damage degrees based on UPV measurement perpendicular to the crack on test surface (3–3 in Fig. 5) and normalised D_{nssm}. These differences can be interpreted by the directions of measurement compared with the direction of cracks. The damage degree can be determined from UPV measurements only if the direction of measurement is perpendicular to the direction of cracks.

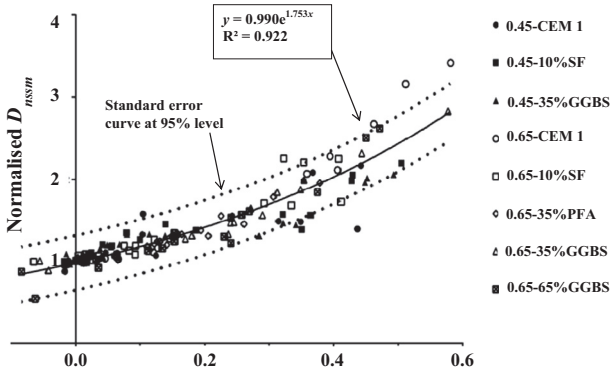

Fig. 17. Relationship between damage degrees based on UPV measured perpendicular to cracks within concrete (transverse direction, i.e. 3–3 in Fig. 5) and normalised D_{nssm}.

The negative values were mainly caused by testing errors, which include the accuracy of test locations and the contact between sensors and test surfaces. However, the negative values were not found at higher load levels, which suggests the sensitivity of UPV test increases with increasing width of cracks. The results of the three figures suggest that the test direction of UPV method should be carefully chosen in order to detect the cracks.

4. Conclusions

From the above results and discussions, the following conclusions have been drawn:

(1) Compressive stresses in concrete can increase the ingress of chloride. Design stresses below 50% f_u do not detrimentally reduce the concrete's resistance to chloride ingress. However, overloading should be avoided because it can cause significant increases in the ingress of chloride ions into the concrete. Concrete in aggressive environments with service loading of over 50% f_u can have a 2–4 times higher chloride migration coefficients compared to concrete without loading.

(2) Significant difference can be found in chloride resistance of concrete under loading and after unloading (load was removed). The chloride migration coefficient of concrete under loading at 75% f_u can be reduced by half if the load is released. This indicates that there are two different situations of chloride ingress in concrete which are under live load as well as under cyclic load. Accidental loading is therefore unlikely to cause a lasting detrimental effect.

(3) Micro-cracks caused by service loads should be taken into account during durability design and service life prediction. The chloride migration coefficient of concrete under loading is different and can be significantly higher than that without loading. Thus a multiplier should be applied to take account of the effect of loading. The findings of this research have indicated that the afore mentioned factor is a function of water/binder (w/b), stress level, mineral additives (ma) and binder content (cc). Further work needs to be carried out to quantify the relative effect of each of these factors.

(4) In the context of all the data presented in this paper, the use of mineral additives such as GGBS would appear to be very effective in extending the service life of structures.

Acknowledgements

The authors gratefully acknowledge funding from the Engineering and Physical Sciences Research Council, UK for the UK-China Bridge in Sustainable Energy and Built Environment (EP/G042594/1) and China Scholarship Council are greatly appreciated. The authors also acknowledge the Life-365 Consortium for providing the software Life-365.

References

[1] W.A. Al-Khaja, Influence of temperature, cement type and level of concrete consolidation on chloride ingress in conventional and high-strength concretes, Constr. Build. Mater. 11 (1997) 9–13.
[2] F. Leng, N. Feng, X. Lu, An experimental study on the properties of resistance to diffusion of chloride ions of fly ash and blast furnace slag concrete, Cem. Concr. Res. 30 (2000) 989–992.
[3] M.D.A. Thomas, P.B. Bamforth, Modelling chloride diffusion in concrete: effect of fly ash and slag, Cem. Concr. Res. 29 (1999) 487–495.
[4] W. Sun, Y. Zhang, S. Liu, Y. Zhang, The influence of mineral admixtures on resistance to corrosion of steel bars in green high-performance concrete, Cem. Concr. Res. 34 (2004) 1781–1785.
[5] Z. Yang, H. Fischer, R. Polder, Laboratory investigation of the influence of two types of modified hydrotalcites on chloride ingress into cement mortar, Cement Concr. Compos. 58 (2015) 105–113.
[6] D.P. Bentz, O.M. Jensen, A.M. Coats, F.P. Glasser, Influence of silica fume on diffusivity in cement-based materials: I. Experimental and computer modeling studies on cement pastes, Cem. Concr. Res. 30 (2000) 953–962.
[7] D. McPolin, P.A.M. Basheer, A.E. Long, K.T.V. Grattan, T. Sun, Obtaining progressive chloride profiles in cementitious materials, Constr. Build. Mater. 19 (2005) 666–673.
[8] A. Petcherdchoo, Time dependent models of apparent diffusion coefficient and surface chloride for chloride transport in fly ash concrete, Constr. Build. Mater. 38 (2013) 497–507.
[9] M.D.A. Thomas, R.D. Hooton, A. Scott, H. Zibara, The effect of supplementary cementitious materials on chloride binding in hardened cement paste, Cem. Concr. Res. 42 (2012) 1–7.
[10] N. Gowripalan, V. Sirivivatnanon, C. Lim, Chloride diffusivity of concrete cracked in flexure, Cem. Concr. Res. 30 (2000) 725–730.
[11] P.P. Win, M. Watanabe, A. Machida, Penetration profile of chloride ion in cracked reinforced concrete, Cem. Concr. Res. 34 (2004) 1073–1079.
[12] S.Y. Jang, B.S. Kim, B.H. Oh, Effect of crack width on chloride diffusion coefficients of concrete by steady-state migration tests, Cem. Concr. Res. 41 (2011) 9–19.
[13] A. Djerbi, S. Bonnet, A. Khelidj, V. Baroghel-Bouny, Influence of traversing crack on chloride diffusion into concrete, Cem. Concr. Res. 38 (2008) 877–883.
[14] M. Ismail, A. Toumi, R. François, R. Gagné, Effect of crack opening on the local diffusion of chloride in cracked mortar samples, Cem. Concr. Res. 38 (2008) 1106–1111.
[15] M. Ismail, A. Toumi, R. Francois, R. Gagne, Effect of crack opening on the local diffusion of chloride in inert materials, Cem. Concr. Res. 34 (2004) 711–716.
[16] H.R. Samaha, K.C. Hover, Influence of micro-cracking on the mass transport properties of concrete, ACI Mater. J. 89 (1992) 416–424.
[17] M. Sahmaran, Effect of flexure induced transverse crack and self-healing on chloride diffusivity of reinforced mortar, J. Mater. Sci. 42 (2007) 9131–9136.
[18] O.G. Rodriguez, R.D. Hooton, Influence of cracks on chloride ingress into concrete, ACI Mater. J. 100 (2003).
[19] M. Sahmaran, I.Ö. Yaman, Influence of transverse crack width on reinforcement corrosion initiation and propagation in mortar beams, Can. J. Civ. Eng. 35 (2008) 236–245.
[20] M. Saito, H. Ishimori, Chloride permeability of concrete under static and repeated compressive loading, Cem. Concr. Res. 25 (1995) 803–808.
[21] C. Lim, N. Gowripalan, V. Sirivivatnanon, Micro-cracking and chloride permeability of concrete under uniaxial compression, Cement Concr. Compos. 22 (2000) 353–360.
[22] Horiguchi T. Antoni, N. Saeki, Assessment of chloride penetration into fibre reinforced concrete under loading. 2005 International Congress – Global Construction: Ultimate Concrete Opportunities, 2005, 717–24.
[23] A. Antoni, Chloride penetration into fiber reinforced concrete under static and cyclic compressive loading, Civil Eng. Dimension 10 (2008) 63–69.
[24] H. Wang, C. Lu, W. Jin, Y. Bai, Effect of external loads on the chloride transport in concrete, J. Mater. Civ. Eng. 23 (2011) 1043–1049.
[25] G.P. Li, F.J. Hu, Y.X. Wu, Chloride ion penetration in stressed concrete, J. Mater. Civ. Eng. 23 (2011) 1145–1153.
[26] B. Violetta, Life-365 service life prediction model, Concr. Int. 24 (2002) 53–57.
[27] Life-365™ Consortium II. LIFE-365, service life prediction model, computer program for predicting the service life and life-cycle costs of reinforced concrete exposed to chlorides, Version 2.1., 2012.
[28] P. Bamforth, Enhancing reinforced concrete durability: Part two: Supplementary Technical Reports. Concrete Society Technical Report 61, 2004, 61.
[29] T. Siemes, C. Edvardsen, Duracrete: service life design for concrete structures, in: Eighth International Conference on Durability of Building Materials and Components, 8 dbmc, 1999, 1343–1356.
[30] British Standards Institution. BS EN 1992-1-1:2004, Eurocode 2: Design of concrete structures – Part 1–1: General rules and rules for buildings, 2011.
[31] W.D. Lindquist, D. Darwin, J.A. Browning, G.G. Miller, Effect of cracking on chloride content in concrete bridge decks, ACI Mater. J. 103 (2006) 467–473.
[32] O.E. Gjørv, Durability of reinforced concrete wharves in Norwegian habours, Ingeniørforlaget, Oslo, 1968, p. 208.
[33] British Standards Institution. BS EN 12620:2002 +A1:2008, Aggregates for concrete. British Standards Institution, 2008.
[34] British Standards Institution. BS EN 197-1:2011, Cement Part 1: Composition, specifications and conformity criteria for common cements.
[35] British Standards Institution. BS 6699:1992, Specification for ground granulated blastfurnace slag for use with Portland cement.
[36] British Standards Institution. BS EN 450-1:2005 + A1:2007, Fly ash for concrete—Part 1: Definition, specifications and conformity criteria. British Standards Institution, 2007.
[37] British Standards Institution. BS EN 13263-1:2005+A1:2009, Silica fume for concrete—Part 1: Definitions, requirements and conformity criterial.
[38] British Standards Institution. BS EN 934-2:2009, Admixtures for concrete, mortar and grout. Part 2: Concrete admixtures – Definitions, requirements, conformity, marking and labelling. British Standards Institution, 2009.
[39] British Standards Institution. BS 1881-125:1986 Testing concrete—Part 125: Methods for mixing and sampling fresh concrete in the laboratory.
[40] Nordtest. NT Build 492 Approved 1999-11, Concrete, mortar and cement-based repair materials: Chloride migration coefficient from non-steady-state migration experiments, 1999.
[41] S. Jacobsen, J. Marchand, L. Boisvert, Effect of cracking and healing on chloride transport in OPC concrete, Cem. Concr. Res. 26 (1996) 869–881.
[42] P.K. Mehta, P.J.M. Monteiro, Concrete: Microstructure, Properties, and Materials, 3rd ed., McGraw-Hill, New York, 2006. p. 659.
[43] British Standards Institution. NA to BS EN 1992-1-1:2004, UK National Annex to Eurocode 2: Design of concrete structures – Part 1–1: General rules and rules for buildings, 2009.
[44] N.R. Buenfeld, E. Okundi, Effect of cement content on transport in concrete, Mag. Concr. Res. 50 (1998) 339–351.
[45] W. Zhang, H. Ba, S. Chen, Effect of fly ash and repeated loading on diffusion coefficient in chloride migration test, Constr. Build. Mater. 25 (2011) 2269–2274.
[46] S.V. Nanukuttan, L. Basheer, W.J. McCarter, D.J. Robinson, P.A. Muhammed Basheer, Full-scale marine exposure tests on treated and untreated concretes-initial 7-year results, ACI Mater. J. 105 (2008) 81–87.
[47] P. Bamforth, The derivation of input data for modelling chloride ingress from eight-year UK coastal exposure trials, Mag. Concr. Res. 51 (1999) 87–96.
[48] P.S. Mangat, B.T. Molloy, Prediction of long term chloride concentration in concrete, Mater. Constr. 27 (1994) 338–346.
[49] K. Stanish, M. Thomas, The use of bulk diffusion tests to establish time-dependent concrete chloride diffusion coefficients, Cem. Concr. Res. 33 (2003) 55–62.